Nontrivial Spin Dimer in the Hexagonal Ruthenate $Ba_3CaRu_2O_9$ Revealed by Nonmagnetic Ion Substitution

Daiki Nishihara, Akinori Kimura, Akitoshi Nakano, Hiroki Taniguchi, Ichiro Terasaki

Department of Physics, Nagoya University, Nagoya 464-8601, Japan

We have prepared a set of polycrystalline samples of $Ba_3Ca(Ru_{1-x}Nb_x)_2O_9$ consisting of the face-shared $(Ru,Nb)_2O_9$ dimer block from $x = 0$ to 0.12, and have measured the x-ray diffraction and magnetization. We find that all the samples of $x > 0$ show Curie-Weiss-like susceptibility below 30 K with the Weiss temperature θ_{Nb} of 2–7 K, which suggests that the Nb-substituted $NbRuO_9$ dimer interacts the Ru_2O_9 dimers magnetically. We also find the $NbRuO_9$ dimer effectively works as $S = 1$ in the dilution limit, which is also suggested by the first-principle calculation. The Ru_2O_9 dimer lattice is nontrivial in the sense that $S = 1$ moment in the $NbRuO_9$ dimer is screened for large x without any magnetic long range order. A possible origin is discussed.

1. Introduction

The internal degrees of freedom have been a vital concept in various fields of physics. The spin, charge and orbital degrees of freedom inherent in an electron in solids cooperate in some materials and compete in others, consequently exhibiting a wide variety of ordered states.[1)] Additional internal degrees of freedom can be seen in materials with complicated structures composed of atom/molecule clusters. In some charge-transfer organic salts, for example, a pair of organic molecules behave like one pseudo-ion to show the insulating ground state called "dimer Mott insulator".[2)] This state has offered a strong candidate for quantum spin liquid, and has been extensively investigated for the last decades.[3,4)] The dimer Mott insulator shows dielectric anomaly arising from intra-molecular charge excitation that is not observed in conventional Mott insulators,[5–7)] and sometimes competes with a charge-ordered state.[8)] These typically exemplifies the dimer degrees of freedom.

We have studied complex transition-metal oxides consisting of face-shared oxygen octahedra, and clarified their exotic electronic states by regarding the face-shared oxygen cluster as a multimer of transition-metal ions sitting inside. We proposed that $BaIrO_3$ can be regarded as "trimer Mott insulator" in which one electron is localized in each face-shared Ir_3O_{12} trimer,[9,10)] and explained the phase transition[11,12)] in terms of competing interactions between inter- and intra-trimers. We also suggested that an intra-trimer charge transfer stabilizes the electronic states in $Ba_4Ru_3O_{10}$,[13)] and explained the anomalous magnetic order in this compound.[14)] Streltzov and Khomskii[15)] have explained the experiments theoretically in terms of molecular orbitals in the trimers.

We have recently focused on the hexagonal-perovskite-related ruthenate $Ba_3CaRu_2O_9$, whose crystal structure is schematically shown in Fig. 1(b), where the Ru_2O_9 dimer formed by the two face-shared RuO_6 octahedra is connected to the CaO_6 octahedron in a corner-shared fashion. In the face-shared Ru_2O_9 block, the Ru ion takes the pentavalent state with the electron configuration of $4d^3$. The Ru_2O_9 layer and the CaO_6 layer alternately stack along the c-axis direction to make hexagonal perovskite related structure with space group $P6_3/mmc$. Darriet et al.[16)] first investigated the structure and magnetism of $Ba_3MRu_2O_9$ (M = Ca, Cd, Sr, and Mg), and found the ground state to be nonmagnetic with a spin gap. $Ba_3CaRu_2O_9$ is a related compound to $Ba_3ZnRu_2O_9$ which we propose as a new type of spin liquid material.[17)] Since a subtle change in the strucure drives the system from the nonmagnetic state to the spin liquid, we expect that $Ba_3CaRu_2O_9$ will be unique in comparison with other spin-gapped materials.

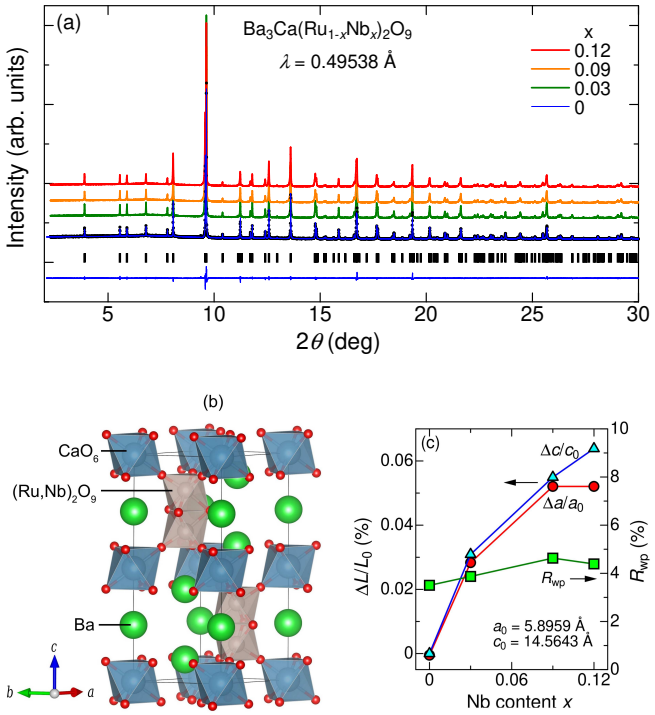

Fig. 1. (Color online) (a) Synchrotron x-ray diffraction patterns of $Ba_3Ca(Ru_{1-x}Nb_x)_2O_9$ (x = 0, 0.03, 0.09, and 0.12) at 300 K and the Rietveld refinement of $x = 0$. (b) Crystal structure of $Ba_3Ca(Ru_{1-x}Nb_x)_2O_9$ drawn using VESTA.[18)] (c) Relative change in the lattice constants ($\Delta L/L_0$) and R factor (R_{wp}) plotted as a function of Nb content x. The lattice constants of $x = 0$ are written as legends.

In this paper, we show how the magnetism of $Ba_3CaRu_2O_9$ is modified by substitution of nonmagnetic Nb^{5+} ions for the magnetic Ru^{5+} ions. We find that Curie-Weiss-like suscepti-

bility systematically shows up with increasing Nb content. By careful analysis, we find that the $NbRuO_9$ dimer works as $S = 1$ in the dilution limit rather than $S = 3/2$ naturally expected from $4d^3$, which can be understood in terms of bonding orbital. We also find that the Weiss temperature is extraordinarily high, which reflects the interaction between the Ru_2O_9 and $NbRuO_9$ dimers. Low-temperature susceptibility normalized by impurity concentration systematically decreases with increasing impurity, and this fact implies that the impurity spins are screened in this particular compound, suggesting that the Ru_2O_9 dimer lattice is nontrivial.

2. Experimental

A set of polycrystalline samples of $Ba_3Ca(Ru_{1-x}Nb_x)_2O_9$ ($0 \le x \le 0.12$) were prepared by solid-state reaction method using high purity powders of $BaCO_3$ (99.99 %), Ru (99.99 %), $CaCO_3$ (99.99 %), and Nb_2O_5 (99.99 %). Stoichiometric amounts of the powders were ground for 30 min, and pressed into pellets at 20 MPa. The pellets were pre-sintered in Al_2O_3 flat crucibles for 12 h at 1273 K in air. After that, the pre-sintered samples were reground for 30 min, repressed into pellets, and sintered in Al_2O_3 boats for 72 h at 1473 K in air. As a supplementary reference, a set of polycrystalline samples of $Ba_3Sr(Ru_{1-x}Nb_x)_2O_9$ ($0 \le x \le 0.12$) were prepared by the same solid-state reaction method using high purity powders of $SrCO_3$ (99.99 %) instead of $CaCO_3$ (99.99 %). The sintering conditions were identical to those of $Ba_3Ca(Ru_{1-x}Nb_x)_2O_9$.

The synchrotron x-ray diffraction (SXRD) measurements were performed at BL02B2 in SPring-8 with a wavelength of 0.49538 Å at 300 K.[19] The diffraction patterns were analyzed using the Rietveld refinement with Jana 2006.[20] The magnetization was measured with a commercial SQUID susceptmeter (Magnetic Property Measurement System, Quantum Design). The temperature dependence of magnetization was measured from 2 to 300 K in an external magnetic field B_{ext} of 1 T and 0.1 T, and the magnetic field dependence of the magnetization was taken from -7 to 7 T at 1.8, 3, 4 and 5 K.

The band calculations were performed for $Ba_3Ca(Ru_{1-x}Nb_x)_2O_9$ ($x = 0$ and 0.12) using AkaiKKR (MACHIKANEYAMA 2002 V009c package).[21] Calculation was performed in the local spin-density approximation based on the parameterization given by Moruzzi, Janak and Williams,[22] and relativistic effect was taken into account on the basis of the scalar relativistic approximation. The lattice parameters of $Ba_3CaRu_2O_9$ were employed from the SXRD data. As a structural model, we used the results analyzed by Wilkens and Müller-Buschbaum.[23] The number of k-points used to calculate the total energy, magnetic moment, and the density of states was set to be 219.

3. Results and discussion

Figure 1 (a) shows the SXRD patterns of $Ba_3Ca(Ru_{1-x}Nb_x)_2O_9$ ($x = 0$, 0.03, 0.06, and 0.12). No impurity phases are detected in all the samples. The lattice constants of $x = 0$ are evaluated to be $a = 5.8959$ Å and $c = 14.5643$ Å, and increase with Nb content x, while the R factor R_{wp} remains a low value of ~ 4% as shown in Fig. 1(c). The increase in the lattice parameters indicates that Nb^{5+} with a larger ionic radius (0.64 Å) successfully replaced Ru^{5+} (0.57 Å).

Figure 2(a) shows the temperature dependence of the susceptibility of $Ba_3Ca(Ru_{1-x}Nb_x)_2O_9$ in 1 T. We only show zero-field-cooled data because no hysteresis was observed between the field-cooling and zero-field-cooling processes. As is similar to the previous studies,[16,24] the magnetic susceptibility for $x = 0$ gradually decreases from room temperature and touches a low value of 8×10^{-5} emu/mol around 35 K. This indicates that a strong antiferromagnetic interaction works within the Ru_2O_9 dimer, and the two Ru spins in the dimer tend to form spin singlet. Senn et al.[24] analysed the temperature dependence of the susceptibility for $x = 0$ in terms of independent spin dimers of $S = 3/2$ with an antiferromagnetic intra-dimer coupling $J_{intra} = 240$ K. Actually, the decrease of the susceptibility becomes remarkable when k_BT is smaller than J_{intra}. Below 35 K, the susceptibility takes an upturn to show a tiny Curie tail, which we ascribe to paramagnetism coming from unwanted impurity contained in the powder source.

Let us have a look at the Nb substitution effects. As shown in Fig. 2(a), the room-temperature susceptibility is almost independent of the Nb content x. This indicates that all the Ru spins are paramagnetic, while the nonmagnetic Nb ions seem

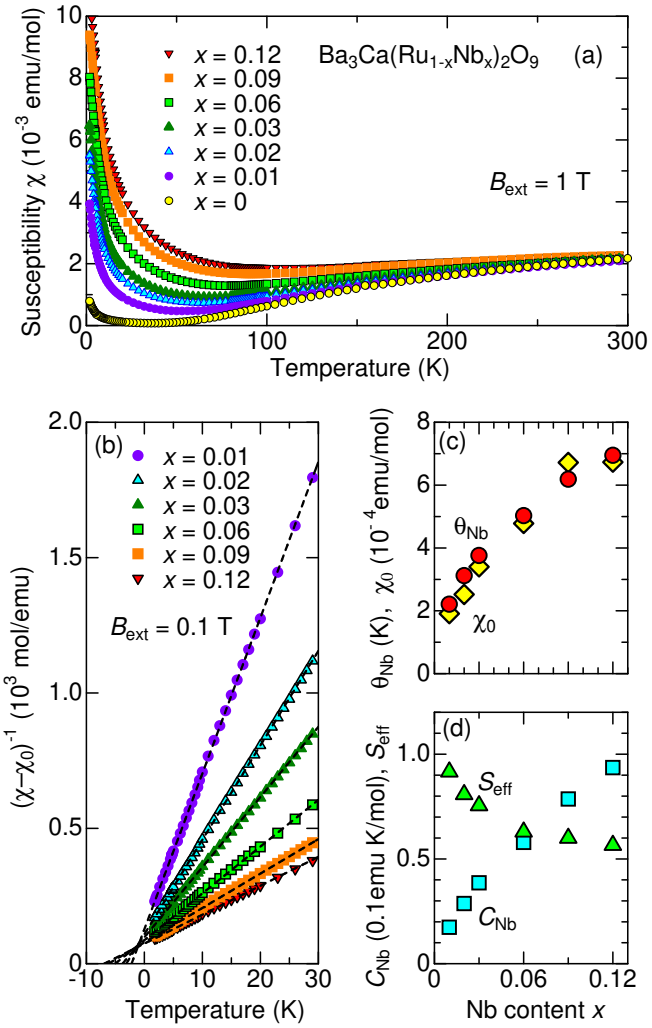

Fig. 2. (Color online) (a) Temperature dependence of the susceptibility in 1 T for $Ba_3Ca(Ru_{1-x}Nb_x)_2O_9$. (b) Temperature dependence of $(\chi-\chi_0)^{-1}$ below 30 K for $Ba_3Ca(Ru_{1-x}Nb_x)_2O_9$. The broken lines show the linear fitting of $(\chi-\chi_0)^{-1} = (T+\theta_{Nb})/C_{Nb}$. (c) The Weiss temperature θ_{Nb} and the constant susceptibility χ_0 obtained from the Curie-Weiss fitting. (d) The Curie constant C_{Nb} and the effective spin S_{eff} calculated from C_{Nb} (see text).

unworking. With decreasing temperature, the susceptibility of $x > 0$ decreases from 300 K similarly to $x = 0$, but the temperature dependence becomes weaker for larger x. Below about 80 K, it takes a significant upturn, which systematically grows with x. Similar Curie tails induced by nonmagnetic substitution are widely observed in antiferromagnetic systems such as spin-dimer lattices,[25–27] Haldane chain,[28] ladder compounds,[29,30] and a spin-Peierls compound.[31,32]

We consider an origin of the Curie tail induced by Nb substitution on the basis of a localized electron picture. When a tiny amount of Nb is introduced ($x \ll 1$), the Nb ion occupies either Ru site in a Ru_2O_9 dimer. We call this "the half-substituted dimer $NbRuO_9$," in which the Ru spin pair is broken up, and the lone Ru ion behaves as a local moment with an effective spin $S_{\rm eff}$. Accordingly, the concentration of the half-substituted dimer $N_{\rm Nb}$ increases with increasing x, and the Curie tail becomes evident. In this respect, the weak x dependence of 300-K susceptibility can be interpreted as an accidental compensation for the dilution effects by the Curie tail.

We fit the susceptibility for $x \geq 0.01$ from 2 to 35 K in 0.1 T by

$$\chi = \frac{C_{\rm Nb}}{T + \theta_{\rm Nb}} + \chi_0, \qquad (1)$$

where $C_{\rm Nb}$, $\theta_{\rm Nb}$ and χ_0 are, respectively, the Curie constant, the Weiss temperature and the constant susceptibility associated with the half-substituted dimer $NbRuO_9$. Although Nb is nonmagnetic, we use the subscript 'Nb' meant for $NbRuO_9$ in $C_{\rm Nb}$ and $\theta_{\rm Nb}$ in order to distinguish the Ru_2O_9 dimers. Figure 2(b) shows $(\chi - \chi_0)^{-1}$ plotted as a function of temperature below 30 K in 0.1 T. A linear relation of $(\chi - \chi_0)^{-1}$ to T is seen in all the data as denoted by the broken lines, whose slope and intercept correspond to $1/C_{\rm Nb}$ and $\theta_{\rm Nb}$, respectively. The excellent linear relation indicates that the half-substituted dimer works as a localized moment.

The results of the linear fitting are summarized in Figs. 2(c) and (d). Note that χ_0 reflects the magnetism of the host Ru_2O_9 dimers. As shown in Fig. 2(a), the Curie tail for $x \neq 0$ seems to merge into the susceptibility of $x = 0$ above around a certain temperature T^*, and χ_0 represents the susceptibility of $x = 0$ around T^*. Since T^* seems to increase with x, χ_0 also increases with x, which we do not discuss hereafter. $\theta_{\rm Nb}$ is evaluated to be from 2.2 K for $x = 0.01$ to 7.0 K for $x = 0.12$, which gives an estimate of spin-spin interaction. Note that these values are extraordinarily high. In the $x = 0.01$ sample, for example, the average distance between half-substituted dimers is roughly $(100)^{1/3} = 4.6$ in lattice parameter unit, indicating that the value of $\theta_{\rm Nb} = 2.2$ K should be too large if a half-substituted dimer interacted another half-substituted dimer directly beyond several spin singlets of Ru_2O_9 dimers. One possibility is that Ru_2O_9 is not perfectly nonmagnetic as was believed thus far, but the spin correlation mediates from one $NbRuO_9$ to another $NbRuO_9$ through the in-between Ru_2O_9 dimers. Recently Asai et al.[33] performed an inelastic neutron scattering experiment of $Ba_3CaRu_2O_9$, and found $J_{\rm intra}$ to be 35 meV, and the inter-dimer interaction $J_{\rm inter}$ to be -1.1 meV for the nearest-neighbor (in-layer) dimers and -0.3 meV for the next-nearest-neighbor (cross-layer) dimers. A value of $k_B\theta_{\rm Nb}$ seems to saturate with increasing x (0.8 meV at $x = 0.12$), and comes close towards the in-layer $|J_{\rm inter}|$. This suggests that the $NbRuO_9$ dimer interacts the nearest-neighbor Ru_2O_9 dimers with $J_{\rm inter}$ = -1.1 meV. We also emphasize that there is no long range order for $T \ll \theta_{\rm Nb}$; the susceptibility of x =0.12 with $\theta_{\rm Nb}$ of 7 K shows no anomaly down to 1.8 K. Thus $\theta_{\rm Nb}$ unlikely corresponds to the superexchange energy of local moments.

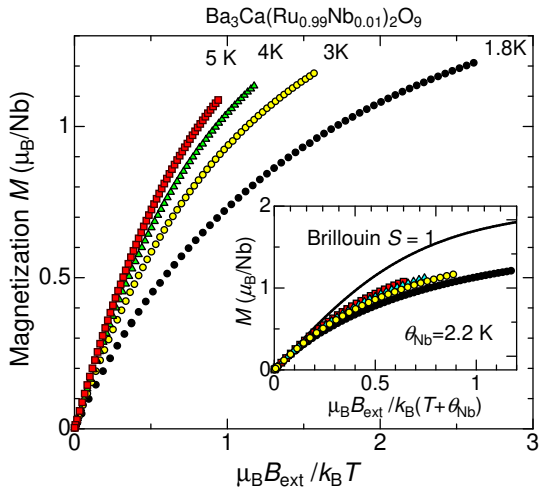

Fig. 3. (Color online) Magnetization plotted as a function of $\mu_{\rm B}B_{\rm ext}/k_{\rm B}T$ at 1.8, 3 , 4, and 5 K for $x = 0.01$. The magnetization plotted as a function of $\mu_{\rm B}B_{\rm ext}/k_{\rm B}(T + \theta_{\rm Nb})$ with Brillouin function of $S = 1$ is shown in the inset.

Now let us evaluate $S_{\rm eff}$ from the Curie constant given by

$$C_{\rm Nb} = \frac{g^2{\mu_{\rm B}}^2}{3k_{\rm B}} N_{\rm Nb} S_{\rm eff}(S_{\rm eff} + 1). \qquad (2)$$

In the low limit of x, Nb impurity is well separated, and the fraction of the half-substituted dimer $NbRuO_9$ equals $2x$. With increasing x, the fully-substituted dimer Nb_2O_9 starts to appear, and does not contribute $N_{\rm Nb}$. The fraction of the fully substituted dimer Nb_2O_9 can be evaluated to be $2x \cdot x = 2x^2$, because Nb_2O_9 : $NbRuO_9 = x : 1$ is expected. Thus we use $N_{\rm Nb} = 2x(1 - x)N_0$, where N_0 is the number of all the dimers per mole. Figure 2(c) shows $C_{\rm Nb}$ and $S_{\rm eff}$ evaluated from Eq. (2). We find that the half-substituted dimer seems to behave as $S = 1$ in the low x limit. This is rather surprising from a localized electron picture, because the lone Ru^{5+} ion taking the $4d^3$ configuration in the $NbRuO_9$ is expected to behave as $S = 3/2$. We further find that $S_{\rm eff}$ decreases gradually with x, which is also difficult to understand within a framework of the simple localized-electron picture. A possible scenario is discussed later.

Figure 3 shows the magnetization plotted against $\mu_{\rm B}B_{\rm ext}/k_{\rm B}T$ at 1.8, 3, 4, and 5 K. The magnetization curves do not follow scaling as a function of $\mu_{\rm B}B_{\rm ext}/k_{\rm B}T$, excluding possibility of non-interacting local moments in the $NbRuO_6$ dimer. When the moments weakly interact, the magnetization curves are known to fall into a scaling curve as a function of $\mu_{\rm B}B_{\rm ext}/k_{\rm B}(T + \theta_{\rm Nb})$.[34,35] As is seen in the inset of Fig. 3, scaling tendency is somewhat cured, but yet all the data systematically deviate at high fields. The black curve represents the Brillouin function for $S = 1$, which is in reasonable agreement with the experimental data at $\mu_{\rm B}B_{\rm ext}/k_{\rm B}T \sim 0$. Note that the magnetization seems to approach to a certain value larger than $1\mu_B$ ($S = 1/2$) in the high field limit; this is another piece of evidence that $S_{\rm eff}$ is

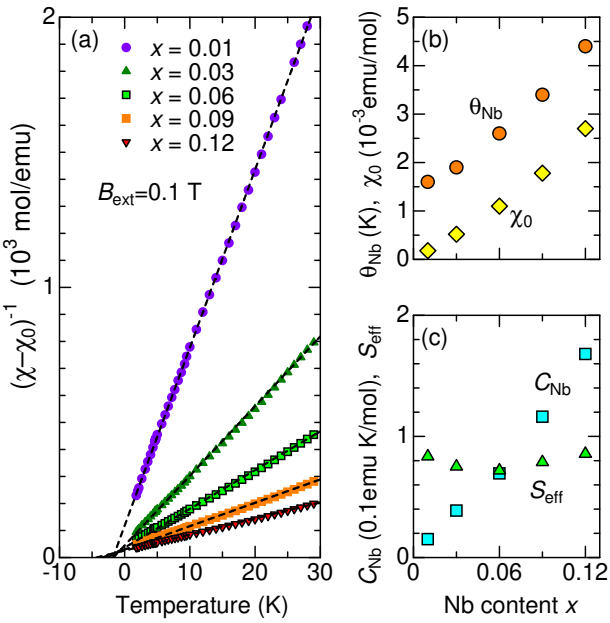

Fig. 4. (Color online) (a) Temperature dependence of $(\chi - \chi_0)^{-1}$ below 30 K for $Ba_3Sr(Ru_{1-x}Nb_x)_2O_9$. The broken lines show the linear fitting of $(\chi - \chi_0)^{-1} = (T + \theta_{Nb})/C_{Nb}$. (b) The Weiss temperature θ_{Nb} and the constant susceptibility χ_0 obtained from the Curie-Weiss fitting. (c) The Curie constant C_{Nb} and the spin size S_{eff} calculated from C_{Nb}.

Table I. Calculated total energies and magnetic moment in $Ba_3Ca(Ru_{1-x}Nb_x)_2O_9$ ($x = 0$ and 0.12)

x	Total Energy (Ry)	Total Moment (μ_B/u.c.)	Ru Moment (μ_B/Ru)	O Moment (μ_B/O)
0	-139154.90371895	11.7104	1.81815	0.13694
0.12	-138473.56976484	9.8886	1.89275	0.09556

close to 1 rather than 1/2 or 3/2.

Here we compare the data in Fig. 2 with the susceptibility of $Ba_3SrRu_2O_9$ shown in Fig. 4. Since Sr has a larger ionic radius than Ca, the lattice parameters (the inter-dimer distance) are larger in $Ba_3SrRu_2O_9$ (a = 5.9614 Åand c = 15.0129 Å), and the structure is distorted (with the space group $C2/c$) possibly because of too large ion size of Sr.[36] Aside from these, the ground state is believed to be nonmagnetic with a finite spin gap similarly to $Ba_3CaRu_2O_9$. As expected, Nb substitution induces similar Curie-Weiss-like susceptibility at low temperatures (Fig. 4(a)). The data are analysed by Eq. (1), and the results are shown in Figs. 4(b) and (c). The fitted values are close to those in Fig. 2; the Weiss temperature θ_{Nb} is slightly lower because of the longer inter-dimer distance. S_{eff} is around 0.9 for $x = 0.01$, consolidating the half-substituted dimer behave as $S = 1$.

Next, we will discuss the band calculations. Table 1 summarizes the results for $Ba_3Ca(Ru_{1-x}Nb_x)_2O_9$ ($x = 0$ and 0.12). The increase in the total energy from $x = 0$ to 0.12 reflects the instability due to the Nb substitution. Note that the number of Ru moment is about 1.8 μ_B, being close to 2 μ_B ($S = 1$). This suggests that the spin of Ru^{5+} behaves as $S = 1$ and the same electronic state is maintained in $x = 0.12$.

Figure 5 shows the density of states (DOS) for $Ba_3Ca(Ru_{1-x}Nb_x)_2O_9$ ($x = 0$ and 0.12), where 0 eV corresponds to the Fermi energy. The upper [lower] half of the figure corresponds to the DOS for up [down] spins. The gross features are consistent with the previous band calculation in the related compound $Ba_3CoRu_2O_9$ by Streltsov,[37] who has found that Ru 4d orbitals strongly hybridize in the Ru_2O_9 dimer, and the bonding orbital of a_{1g} character is formed to accept two 4d electrons per dimer. As a result, S_{eff} is reduced from 3/2 to 1 per Ru^{5+}. The same thing happens even for $x = 0.12$ in our calculation; this is reasonable because our calculation is based on coherent potential approximation in which a fictitious atom of $Ru_{0.88}Nb_{0.12}$ is assumed in a self-consistent manner. Streltsov and Khomskii[38] have pointed out that similar bonding-orbital formation essentially affects the magnetism in various transition metal oxides. Zhou et al. have suggested the $S = 1$ state in the Ru^{5+} in $Ba_3CoRu_2O_9$ at low temperatures.[39]

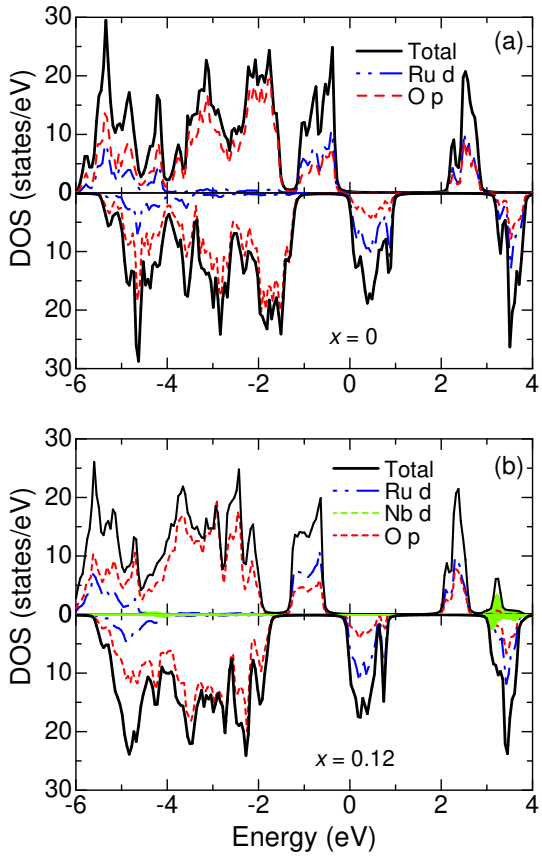

Fig. 5. (Color online) The calculated total and partial density of states in $Ba_3Ca(Ru_{1-x}Nb_x)_2O_9$ ($x = 0$ and 0.12)

Finally we compare the present compound with other magnetic systems. An antiferromagnetic order has been often induced by doping nonmagnetic ions in spin-gapped materials such as the spin-Peierls compound $CuGeO_3$,[31,32,40,41] the spin-ladder compound $SrCu_2O_3$,[29] the Haldane-gap compound $PbNi_2V_2O_8$,[28] and the spin-dimer compound $TlCuCl_3$,[25] known as "order from disorder."[42] In these compounds, an antiferromagnetic long-range order competes with the spin-gap state. By doping nonmagnetic impurities, competing long-range spin-spin correlation grows, and sometimes coexists with the spin-gapped state. Such situations have been theoretically investigated by many researchers.[43–47] On the other hand, impurity ions do not induce long-range or-

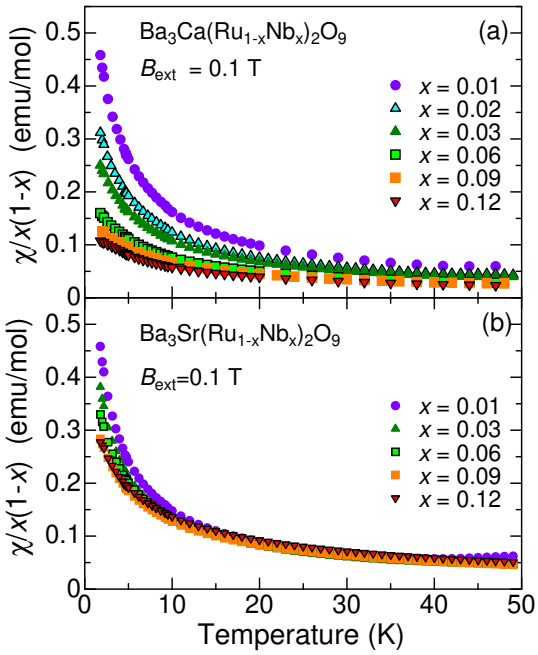

Fig. 6. (Color online) Susceptibility normalized by the $NbRuO_9$ concentration ($\chi/x(1-x)$) for (a) $Ba_3Ca(Ru_{1-x}Nb_x)_2O_9$ and (b) $Ba_3Sr(Ru_{1-x}Nb_x)_2O_9$.

der in other spin-gapped compounds such as the organic Haldane-gap material NENP,[48] the spin-ladder compound $BiCu_2PO_6$,[30] and the spin-dimer compound $Ba_3M_2O_8$ (M = Cr and Mn),[26,27] possibly owing to the lack of competing antiferromagnetic orders. The lack of long range order may be used for long-distance entanglement essential to quantum teleportation, as suggested in $Sr_{14}Cu_{24}O_{41}$.[49] Although the present material does not show magnetic order at $T \ll \theta_{Nb}$, it possesses two unique features: (i) the Weiss temperature increases with impurity concentration, and (ii) the effective spin number decreases with impurity concentration.

These two features imply that the magnitude of the susceptibility normalized by the $NbRuO_9$ concentration decreases with increasing impurity concentration at the lowest temperature, suggesting that the moment in the $NbRuO_9$ is screened by the Ru_2O_9 dimer lattice. In a spin-ladder system, Motome et al.[45] speculated that the ground state may change from spin-gapped state to spin liquid with increasing nonmagnetic impurity. In such a spin-liquid state, where spin-singlet pairs dynamically fluctuate to recompose the pair partners, the impurity-induced spins are screened by contributing to the fluctuating singlet pairs. Since the spin ladder can be regarded as a one-dimensional dimer lattice, we expect that a similar phenomenon may happen in a two-dimensional dimer lattice.

Figure 6 (a) shows the susceptibility normalized by the $NbRuO_9$ concentration ($\chi/x(1-x)$) for $Ba_3Ca(Ru_{1-x}Nb_x)_2O_9$. Clearly, the data systematically decrease with x, and the data for $x = 0.12$ show nearly flat temperature dependence, suggesting screened magnetism. In such situations, the Weiss temperature in Eq. (1) corresponds to the strength of spin fluctuation[50,51] rather than J_{inter}. As the $NbRuO_9$ dimers increase, the magnetization and spin fluctuation increase to destabilize the spin-singlet state. The external fields also increase the magnetization to destabilize the spin-singlet state, and accordingly the screening scenario can explain the high-field suppression of the magnetization shown in Fig. 3. Yamamoto et al.[34] found similar tendency in the low-temperature susceptibility in $Ba_3Zn_{1-x}M_xRu_2O_9$ (A = Zn; M = Co, Ni, Cu), and pointed out that the local magnetic moment in the M ion is screened by the Ru_2O_9 dimer lattice. In the case of $Ba_3Sr(Ru_{1-x}Nb_x)_2O_9$, where the Ru_2O_9 dimers are well separated, $\chi/x(1-x)$ is nearly dependent of x (Fig. 6(b)), indicating that the $NbRuO_9$ moments are unscreened.

Very recently, an exotic magnetic state has been theoretically suggested in a S=1 dimer lattice by Tanaka and Hotta,[52] where the spin-singlet phase is smoothly evolved into a quadrupolar spin liquid phase with increasing interdimer interaction. If the quadrupolar spin liquid is realized in the related compound $Ba_3ZnRu_2O_9$, it will not be surprising that unconventional impurity effects are observed in the title compound as a precursor to the quadrupolar spin liquid. Such an exotic state comes from fourth-order process based on a bilinear–biquadratic Hamiltonian,[53,54] and the parameters used in the Hamiltonian should be evaluated with real experiments.

4. Summary

We have measured synchrotron x-ray diffraction and magnetization for a set of polycrystalline samples of $Ba_3Ca(Ru_{1-x}Nb_x)_2O_9$ and $Ba_3Sr(Ru_{1-x}Nb_x)_2O_9$, and discussed the non-magnetic impurity substitution effects to the spin-dimer lattice consisting of face-shared Ru_2O_9 octahedra. From the x-ray diffraction measurements, we find that the lattice parameters increase with x, indicating the Nb ions were successfully substituted for the Ru site. In the magnetization measurement, the $NbRuO_9$ dimer behaves as paramagnetic spin $S = 1$ with the Weiss temperature of a few K in the dilution limit. We suggest that the Ru_2O_9 dimers are not perfectly nonmagnetic, but weakly interact with each other to mediate the interaction between the $NbRuO_9$ dimers. According to the band calculation that we performed, the bonding orbital of a_{1g} character is formed in the dimer, and thereby the effective spin of Ru is close to $S = 1$. We find that the Ru_2O_9 dimer lattice is nontrivial in the sense that the susceptibility normalized by impurity concentration systematically decreases with increasing impurity concentration accompanied by the lack of long-range magnetic order. We suggest that the magnetism of the impurity spins is screened by the Ru_2O_9 dimer lattice, being a precursor to the spin liquid in $Ba_3ZnRu_2O_9$.

Acknowledgements

The authors would like to thank Y. Yasui, C. Hotta, S. Asai, T. Masuda, and T. D. Yamamoto for collaboration and discussion. This study was partially supported by Grant-in-Aid for Scientific Research (Kakenhi No. 18H01173, 19H05791) by MEXT. The synchrotron radiation experiments at the BL02B2 beamline of the SPring-8 facility were conducted with the approval of the Japan Synchrotron Radiation Research Institute (JASRI) (Proposal No. 2019B1089). The data that support the findings of this study are available from the corresponding author upon reasonable request.

*Corresponding author: Ichiro Terasaki (terra@nagoya-u.jp)

1) E. Dagotto: Science **309** (2005) 257.
2) K. Kanoda: Hyperfine Interact. **104** (1997) 235.
3) Y. Shimizu, K. Miyagawa, K. Kanoda, M. Maesato, and G. Saito: Phys. Rev. Lett. **91** (2003) 107001.
4) T. Itou, A. Oyamada, S. Maegawa, M. Tamura, and R. Kato: J. Phys.: Condens. Mat. **19** (2007) 145247.
5) M. Abdel-Jawad, I. Terasaki, T. Sasaki, N. Yoneyama, N. Kobayashi, Y. Uesu, and C. Hotta: Phys. Rev. B **82** (2010) 125119.
6) C. Hotta: Phys. Rev. B **82** (2010) 241104.
7) M. Naka and S. Ishihara: J. Phys. Soc. Jpn. **79** (2010) 063707.
8) R. Okazaki, Y. Ikemoto, T. Moriwaki, T. Shikama, K. Takahashi, H. Mori, H. Nakaya, T. Sasaki, Y. Yasui, and I. Terasaki: Phys. Rev. Lett. **111** (2013) 217801.
9) I. Terasaki, S. Ito, T. Igarashi, S. Asai, H. Taniguchi, R. Okazaki, Y. Yasui, K. Kobayashi, R. Kumai, H. Nakao, and Y. Murakami: Crystals **6** (2016).
10) R. Okazaki, S. Ito, K. Tanabe, H. Taniguchi, Y. Ikemoto, T. Moriwaki, and I. Terasaki: Phys. Rev. B **98** (2018) 205131.
11) T. Siegrist and B. Chamberland: J. Less Common Metals **170** (1991) 93.
12) G. Cao, J. Crow, R. Guertin, P. Henning, C. Homes, M. Strongin, D. Basov, and E. Lochner: Solid State Commun. **113** (2000) 657.
13) T. Igarashi, Y. Nogami, Y. Klein, G. Rousse, R. Okazaki, H. Taniguchi, Y. Yasui, and I. Terasaki: J. Phys. Soc. Jpn. **82** (2013) 104603.
14) Y. Klein, G. Rousse, F. Damay, F. Porcher, G. André, and I. Terasaki: Phys. Rev. B **84** (2011) 054439.
15) S. V. Streltsov and D. I. Khomskii: Phys. Rev. B **86** (2012) 064429.
16) J. Darriet, M. Drillon, G. Villeneuve, and P. Hagenmuller: J. Solid State Chem. **19** (1976) 213 .
17) I. Terasaki, T. Igarashi, T. Nagai, K. Tanabe, H. Taniguchi, T. Matsushita, N. Wada, A. Takata, T. Kida, M. Hagiwara, K. Kobayashi, H. Sagayama, R. Kumai, H. Nakao, and Y. Murakami: J. Phys. Soc. Jpn. **86** (2017) 033702.
18) K. Momma and F. Izumi: J. Appl. Crystallogr. **44** (2011) 1272.
19) E. Nishibori, M. Takata, K. Kato, M. Sakata, Y. Kubota, S. Aoyagi, Y. Kuroiwa, M. Yamakata, and N. Ikeda: J. Phys. Chem. Solids **62** (2001) 2095 .
20) V. Petrícek, M. Dusek, and L. Palatinus: Z. Kristallogr. **229** (2014) 345.
21) H. Akai: Hyperfine Interact. **68** (1992) 3.
22) V. Moruzzi, J. Janak, and A. Williams: *Calculated Electronic Properties of Metals* (Pergamon, 1976).
23) J. Wilkens and H. Müller-Buschbaum: J. Alloys Comp. **177** (1991) L31.
24) M. S. Senn, A. M. Arevalo-Lopez, T. Saito, Y. Shimakawa, and J. P. Attfield: J. Phys.: Condens. Matter **25** (2013) 496008.
25) A. Oosawa, T. Ono, and H. Tanaka: Phys. Rev. B **66** (2002) 020405.
26) E. C. Samulon, M. C. Shapiro, and I. R. Fisher: Phys. Rev. B **84** (2011) 054417.
27) T. Hong, L. Y. Zhu, X. Ke, V. O. Garlea, Y. Qiu, Y. Nambu, H. Yoshizawa, M. Zhu, G. E. Granroth, A. T. Savici, Z. Gai, and H. D. Zhou: Phys. Rev. B **87** (2013) 144427.
28) Y. Uchiyama, Y. Sasago, I. Tsukada, K. Uchinokura, A. Zheludev, T. Hayashi, N. Miura, and P. Böni: Phys. Rev. Lett. **83** (1999) 632.
29) M. Azuma, Y. Fujishiro, M. Takano, M. Nohara, and H. Takagi: Phys. Rev. B **55** (1997) R8658.
30) L. K. Alexander, J. Bobroff, A. V. Mahajan, B. Koteswararao, N. Laflorencie, and F. Alet: Phys. Rev. B **81** (2010) 054438.
31) M. Hase, I. Terasaki, Y. Sasago, K. Uchinokura, and H. Obara: Phys. Rev. Lett. **71** (1993) 4059.
32) S. B. Oseroff, S.-W. Cheong, B. Aktas, M. F. Hundley, Z. Fisk, and L. W. Rupp, Jr.: Phys. Rev. Lett. **74** (1995) 1450.
33) S. Asai, A. Kimura, T. Yamamoto, A. Nakano, H. Taniguchi, I. Terasaki, and T. Masuda: JPS 2020 Autumn Meeting (in Japanese) (2020).
34) T. D. Yamamoto, H. Taniguchi, and I. Terasaki: J. Phys.: Condens. Matter **30** (2018) 355801.
35) F. Bert, S. Nakamae, F. Ladieu, D. L'Hôte, P. Bonville, F. Duc, J.-C. Trombe, and P. Mendels: Phys. Rev. B **76** (2007) 132411.
36) H. W. Zandbergen and D. J. W. IJdo: Acta Crystallogr. C **40** (1984) 919.
37) S. V. Streltsov: Phys. Rev. B **88** (2013) 024429.
38) S. V. Streltsov and D. I. Khomskii: PNAS **113** (2016) 10491.
39) H. D. Zhou, A. Kiswandhi, Y. Barlas, J. S. Brooks, T. Siegrist, G. Li, L. Balicas, J. G. Cheng, and F. Rivadulla: Phys. Rev. B **85** (2012) 041201.
40) K. Manabe, H. Ishimoto, N. Koide, Y. Sasago, and K. Uchinokura: Phys. Rev. B **58** (1998) R575.
41) L. P. Regnault, J. P. Renard, G. Dhalenne, and A. Revcolevschi: Europhys. Lett. **32** (1995) 579.
42) Villain, J., Bidaux, R., Carton, J.-P., and Conte, R.: J. Phys. France **41** (1980) 1263.
43) H. Fukuyama, T. Tanimoto, and M. Saito: J. Phys. Soc. Jpn. **65** (1996) 1182.
44) H. Fukuyama, N. Nagaosa, M. Saito, and T. Tanimoto: J. Phys. Soc. Jpn. **65** (1996) 2377.
45) Y. Motome, N. Katoh, N. Furukawa, and M. Imada: J. Phys. Soc. Jpn. **65** (1996) 1949.
46) G. B. Martins, M. Laukamp, J. Riera, and E. Dagotto: Phys. Rev. Lett. **78** (1997) 3563.
47) C. Yasuda, S. Todo, M. Matsumoto, and H. Takayama: Phys. Rev. B **64** (2001) 092405.
48) M. Hagiwara, K. Katsumata, I. Affleck, B. I. Halperin, and J. P. Renard: Phys. Rev. Lett. **65** (1990) 3181.
49) S. Sahling, G. Remenyi, C. Paulsen, P. Monceau, V. Saligrama, C. Marin, A. Revcolevschi, L. P. Regnault, S. Raymond, and J. E. Lorenzo: Nat. Phys. **11** (2015) 255.
50) Y. Takahashi and K. Usami: Journal of the Physical Society of Japan **51** (1982) 2450.
51) K. D. Gross, D. Riegel, and R. Zeller: Phys. Rev. Lett. **65** (1990) 3044.
52) K. Tanaka and C. Hotta: Phys. Rev. B **101** (2020) 094422.
53) K. Tanaka, Y. Yokoyama, and C. Hotta: J. Phys. Soc. Jpn. **87** (2018) 023702.
54) Y. Yokoyama and C. Hotta: Phys. Rev. B **97** (2018) 180404.